

INTRODUCTION

In this study we assess the temporal noise properties of fMRI across different tissue types and brain structures using data collected from four scanners as part of the functional Biomedical Informatics Research Network (fBIRN, www.birn.net) project. The purpose of this study is to help elucidate the sources of noise in fMRI and how they affect different parts of the brain as well as to establish objective criteria for scanner performance. The key innovation here is the decomposition of temporal noise into physiological, thermal, and instability components using human and agar data collected at two flip angles. We find that the physiological noise variance differs substantially across structure but not site, that thermal noise does differ across site, and that the stability performance of all the scanners in the study was excellent.

Sources of fMRI Noise

The temporal noise at a voxel is comprised of several components. For this work we consider the three shown in Table 1: Thermal, Scanner Instability, and Physiological.

Thermal Noise is noise created by the movement of charged particles (ions) near the scanner acquisition coil. It is present whenever the object is above 0°K. It is independent of the amount of signal, meaning that it does not change as the flip angle, TE, or TR change. Thermal noise may also emanate from the electronics or from some external source.

Scanner Instability is the fluctuation in intensity due to shot-to-shot changes in RF transmission and/or gradient waveform (possibly due to power supply), loose hardware, or an external magnetic field source (eg, subway power line).

Physiological Noise is a result of changes in the subject. These may include fluctuations in unmodeled neural responses, oxygen consumption, respiration, heart rate, CSF pulsation, and bulk head motion. Note that, unlike [2], we lump both BOLD-related and BOLD-unrelated physiological noise together.

Table 1: Types of fMRI Temporal Noise

Noise Type	Human	Phantom	Scanner Dependent	Signal Dependent (SD)	Spatial Distribution	Stimulus Correlated
Thermal	Yes	Yes	Yes	No	Uniform	No
Scanner Instability	Yes	Yes	Yes	Yes	Non-uniform	No
Physiological	Yes	No	No	Yes	Non-uniform	Maybe

Theory of Noise Decomposition

Following [2], we model the total variance at a voxel as a linear sum of **Signal-Dependent (SD)** variance and thermal variance (Equations 1 and 2). A simple sum is appropriate because they are independent. The SD component is always there, but its magnitude is dependent on how the data are acquired. The SD component is dependent on the flip angle whereas the thermal component is not. According to the Bloch equations, the factor (M_{10} in Equation 2) by which the SD variance changes with flip angle is proportional to the square of the ratio of sines of the flip angles (Equation 3), which is equal to the square of the ratio of mean intensities (Equation 3). So, if we measure the total variance and mean intensities at two flip angles (77° and 10°), we can compute the amount of variance due to the SD and Thermal components. Using the measured mean intensities is preferable to the theoretical sine of the flip angle as the nominal flip angle set at the scanner console may not be accurate. Finally, we note that the SD noise can be decomposed into physiological noise and instability noise (Equation 4). While both are present in a human, only instability is present in a phantom.

$$\sigma_{77}^2 = \sigma_{SD77}^2 + \sigma_T^2 \quad (1)$$

$$\sigma_{10}^2 = \frac{\sigma_{SD77}^2}{M_{10}^2} + \sigma_T^2 \quad (2)$$

$$M_{10} = \frac{(\sin(77))}{(\sin(10))} = \left(\frac{\mu_{77}}{\mu_{10}}\right)^2 \quad (3)$$

$$\sigma_{SD77}^2 = \sigma_{Phys77}^2 + \sigma_{Inst77}^2 \quad (4)$$

$$\sigma_{Rel}^2 = \frac{\sigma_{SD77}^2}{\mu_{77}^2} \quad (5)$$

$$\sigma_{Abs}^2 = \frac{\sigma_{SD77}^2}{\mu_{WM77}^2} \quad (6)$$

$$SFNR = \sqrt{\frac{1}{\sigma_{Rel}^2}} \quad (7)$$

$\sigma_{77}^2, \sigma_{10}^2$ - Total variance measured at 77° and 10°

σ_{SD77}^2 - Signal Dependent (SD) variance at 77°

σ_T^2 - Thermal (T) variance at all flip angles

M_{10} - Factor by which SD variance is reduced at 10° relative to 77° , typically about 25.

μ_{77}, μ_{10} - Mean intensity measured at 77° and 10°

σ_{Phys77}^2 - Physiological noise variance at 77°

σ_{Inst77}^2 - Instability noise variance at 77°

σ_{Rel}^2 - Relative Variance (scaled by mean intensity² of ROI)

σ_{Abs}^2 - Relative Variance (scaled by WM mean intensity²)

μ_{WM77} - Mean intensity of white matter measured at 77°

SFNR - Signal-to-Fluctuation Noise Ratio [5]

Processing Overview

1. Acquire fMRI data at 10° and 77° (Human and Agar)
2. Compute mean and total variance at each voxel for each flip
3. Average mean and variance within an ROI
4. Solve for SD and Thermal variances using Equations 1-3

Methods Details

Eighteen healthy subjects visited four sites:

1. Duke University
2. Brigham and Woman's Hospital (BWH)
3. Martinos Center, Massachusetts General Hospital (MGH)
4. Yale University (Each subject visited twice)

Human Subject Protocol: each visit consisted of:

- Anatomical scan (MP-RAGE or SPGR)
- fMRI BOLD Rest (10° and 77°)
- fMRI BOLD Task (Not analyzed)
- ASL Rest (Not analyzed)
- B0 map (Not analyzed)

fMRI Protocol: acquisition parameters were matched as closely as possible across sites, though there are some unavoidable differences due to manufacturer (eg, ramp sampling and ghost correction). The site-independent and site-dependent parameters are given in Tables 1 and 2, respectively.

Agar Phantom Protocol: In addition to human scans, each site scanned an agar phantom weekly using the same fMRI protocol (10° and 77°) as was used for the humans. The agar phantom is a sphere with diameter 17.5cm and is designed to have comparable T1 and T2 to that of gray matter [5].

Human Anatomical Analysis: performed using FreeSurfer to extract the cortical surface as well as surface and subcortical regions of interest (ROIs) uniquely defined for each subject. Figure 3.

Human Rest fMRI Analysis

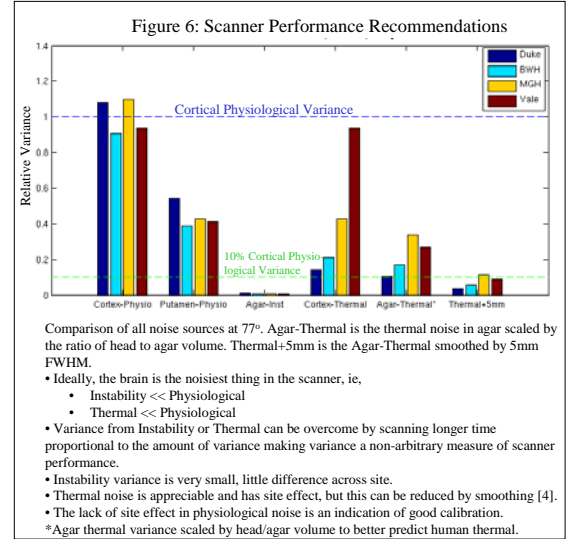
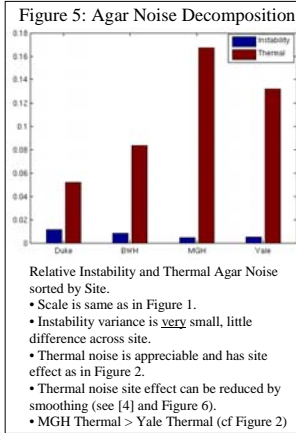
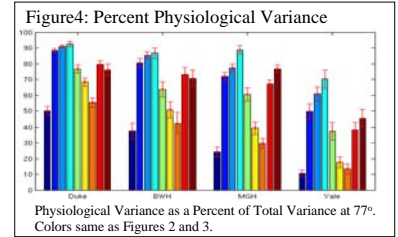
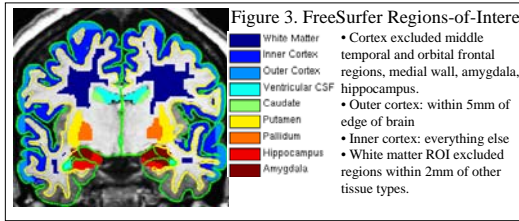
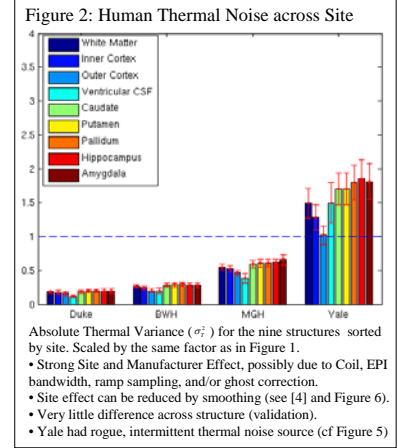
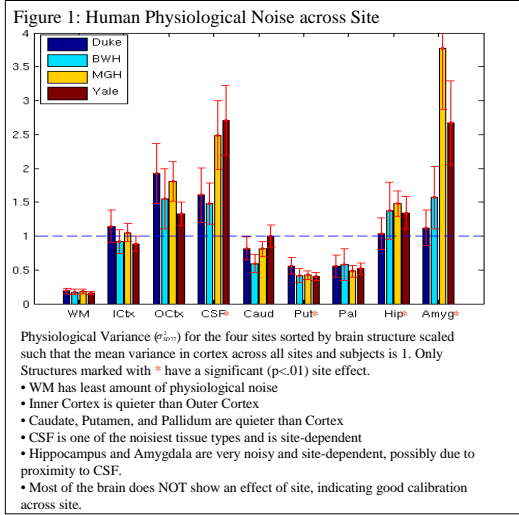
- 10° and 77° Rest data from 8 subjects were analyzed
- Motion correction to the middle time point (AFNI 3dVolReg)
- No spatial smoothing or intensity normalization was applied.
- A GLM was fit to each voxel's time course using
 - 2nd order polynomial and
 - Motion correction parameters as regressors.
- The middle time point was registered to the anatomical space of that subject using SPM.
- Mean image and GLM residual variance mapped to anatomical space
- The mean and variance were averaged inside each ROI.
- The variance of the thermal and physiological noise was then computed in each ROI using the means and variances from both flip angles as described above (Equations 1-3).

Agar fMRI Analysis (10° and 77°): proceeded in a similar manner to the human analysis, except no motion correction was performed. The voxels in the phantom were determined by running the FS_LBET program on the agar volume, and then eroding the mask by 5 voxels to use only the core of the agar.

Table 2: Site Independent fMRI Acquisition Parameters

Parameter/Field	Duke	BWH	MGH	Yale
Field Strength	3T	3T	3T	3T
k-Space Trajectory	EPI	EPI	EPI	EPI
TR	2000 ms	2000 ms	2000 ms	2000 ms
TE	30 ms	30 ms	30 ms	30 ms
Flip Angle	77° and 10°	77° and 10°	77° and 10°	77° and 10°
Time Points	100 (77)	100 (77)	100 (77)	100 (77)
SL	50 (10)	50 (10)	50 (10)	50 (10)
Voxel Size	3.44 mm	3.44 mm	3.44 mm	3.44 mm
Field-of-View	220 mm	220 mm	220 mm	220 mm
Slice Thickness	5 mm (4 skip 1)	5 mm (4 skip 1)	5 mm (4 skip 1)	5 mm (4 skip 1)
Slices	30	30	30	30
Slice Order	Sequential, Ascending	Sequential, Ascending	Sequential, Ascending	Sequential, Ascending
Orientation	Axial, AC-PC	Axial, AC-PC	Axial, AC-PC	Axial, AC-PC
Coil Combining	Sum of Squares	Sum of Squares	Sum of Squares	Sum of Squares
Spatial Filtering ¹ (Fermi, Elliptical)	Off	Off	Off	Off

¹ The GE sites had gradient distortion correction turned on.



SUMMARY

We have used fMRI acquisitions with multiple flip angles on humans and agar phantoms across multiple sites to assess the relative amount of physiological, thermal, and instability noise across multiple brain structure as part of the fBIRN project.

- fMRI acquisition parameters were matched closely across site (Tables 1 and 2)
- Thermal noise does not vary much across brain structure, as expected.
- Physiological noise varies substantially across structure with gray matter noisier than white
- Physiological noise did not show much of a site effect, indicating good calibration across site
- Thermal noise does show a large site effect. The reason for this effect remains a mystery but may be due to differences in hardware or vendor-specific k-space reconstruction.
- This procedure can be easily implemented at any site that wants to assess scanner performance in this way, and the fBIRN will be making analysis software available for this purpose.

Table 3: Site Dependent fMRI Acquisition Parameters

Parameter/Field	Duke	BWH	MGH	Yale
Manufacturer	GE	GE	Siemens	Siemens
Scanner Model	Signa Excite	Signa HDx	TimTrio	Trio
Scanner Software	12.0	14.0	VB13	VA25
Echo Spacing	492 ms	492 ms	500 ms	490 ms
Bandwidth ¹	500 kHz	500 kHz	294.4 kHz (23080-pixels)	302.7 kHz (23680-pixels)
Coil	8 Chan	8 Chan	12 Chan	8 Chan
Grad Dist Cor	On	On	Off	Off

¹ Bandwidth¹ here refers to raw bandwidth and does take into account filtering or averaging the vendor may apply during k-space reconstruction.

References:

- [1] Weiskopf, R. 1996. Simple Measurement of Scanner Stability for Functional NMR Imaging of Activation in the Brain. MRM 36:643-645
- [2] Klinger G, Glover GH. 2001. The physiological noise in oxygen-sensitive magnetic resonance imaging. Magn. Reson. Med. 46:631-637.
- [3] Friedman L, Glover GH. 2006. Report on a multicenter fMRI quality assurance protocol. JMRI 23: 409.
- [4] Friedman L, Glover G, Krasic D, and Magnotta V. The FIRST VBM. 2006. Reducing interscanner variability of activation in a multicenter fMRI study: Role of smoothing equalization. NeuroImage 32: 1656-1666.
- [5] Friedman L, Glover GH, and the fBIRN Consortium. 2006. Reducing interscanner variability of activation in a multicenter fMRI study: Controlling for signal-to-fluctuation noise ratio (SFNR) differences. NeuroImage 33:471-481.

Acknowledgments: Support for this research was provided in part by the National Center for Research Resources (P41-RR-00705) and the National Cancer Institute (P01-CA100130), the National Institute for Biomedical Imaging and Bioengineering (P01-EB001350) as well as the Medical Ethics and Neuroscience Discovery (MEND) Institute. This research was supported by a grant (R01-DC-000702) to the Functional Imaging Biomedical Informatics Research Network (fBIRN, www.birn.net), that is funded by the National Center for Research Resources (NCRR) at the National Institutes of Health (NIH).